WALL MODELING IN LES OF TRAILING-EDGE FLOW

Meng Wang and Parviz Moin
Center for Turbulence Research
Stanford University/NASA Ames Research Center
Moffett Field, CA 94035, U. S. A.
wangm@stanford.edu moin@stanford.edu

ABSTRACT

Wall models based on turbulent boundary-layer equations and their simpler variants are employed in the LES of turbulent flows past an asymmetric trailing-edge. It is demonstrated that, as first noted by Cabot and Moin (2000), when a RANS type eddy viscosity is used in the wall-layer equations with nonlinear convective terms, its value must be reduced to account for only the unresolved part of the Reynolds stress. A dynamically adjusted mixing-length eddy viscosity is used in the boundary-layer equation model, which is shown to be considerably more accurate than the simpler wall models based on the instantaneous log law. This method predicts low-order velocity statistics in good agreement with those from full LES with resolved wall-layers. The unsteady separation near the trailing-edge is captured correctly, and the prediction of surface pressure fluctuations also shows promise.

INTRODUCTION

Large-eddy simulation (LES) of wall-bounded flows becomes prohibitively expensive at high Reynolds numbers if one attempts to resolve the small but dynamically important vortical structures in the near-wall region. The number of grid points required scales as the square of the friction Reynolds number (Baggett et al., 1997), which is nearly the same as for direct numerical simulation. To circumvent the severe near-wall resolution requirement, LES can be combined with a wall-layer model. In this approach, LES is conducted on a relatively coarse grid designed to resolve the desired outer flow scales. The dynamic effects of the energy-containing eddies in the wall layer (viscous and buffer regions) are determined from a wall model calculation, which provides to the outer flow LES a set of approximate boundary conditions, often in the form of wall shear-stresses.

The simplest wall stress models are analogous to the wall functions commonly used in Reynolds-averaged Navier-Stokes (RANS) approaches. They provide an algebraic relationship between the instantaneous local wall stresses and the tangential velocities at the first off-wall velocity nodes (see, for example, Schumann, 1975; Grötzbach, 1987; Piomelli et al., 1989). In essence, these algebraic models all imply the logarithmic law of the wall for the mean velocity, which is not valid in many complex flows. To incorporate more physics into the model, wall models based on boundary layer approximations have been proposed in recent years (Balaras et al., 1996; Cabot and Moin, 2000). Turbulent boundary-layer (TBL) equations are solved numerically on an embedded near-wall mesh to compute the wall stress. The turbulent eddy viscosity is modeled by a RANS type model, such as the mixing-length model with wall damping. Reasonable success has been achieved in predicting attached flows and flows with fixed separation points, such as the backward facing step flow. Cabot and Moin (2000) found that, in the case of the backward facing step, improved solutions were obtained when the mixing-length eddy viscosity was lowered from the standard RANS value. A dynamic procedure was suggested to determine the suitable model coefficient.

The present work is concerned with the use of wall models in the LES of complex turbulent flows with strong favorable/adverse pressure gradients and incipient separation. Wall models based on TBL equations (Cabot and Moin, 2000) and their simpler variants are employed and extended to carry out LES of turbulent boundary layer flows past an asymmetric trailing-edge. The results are compared with those from the full LES with resolved wall-layers (Wang and Moin, 2000) and the experimental measurements of Blake (1975). In particular, we are interested in determining the predictive capabilities of this hybrid LES/wall-modeling approach for flow separation, surface

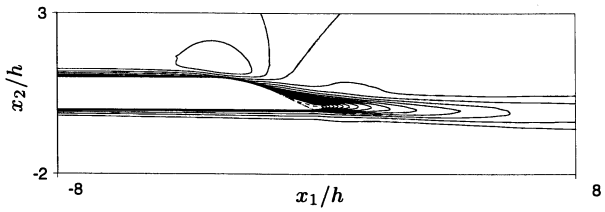

Figure 1: Boundary-layer flow past a trailing-edge. The contours (-0.081 to 1.207 with increment 0.068) represent the mean streamwise velocity normalized by the free-stream value (from Wang and Moin, 2000).

pressure fluctuations, and aerodynamic noise.

The flow configuration is shown in Fig. 1, which depicts contours of the mean streamwise velocity from the full LES of Wang and Moin (2000). The chord Reynolds number is 2.15×10^6, and the trailing-edge tip-angle is 25 degrees. In the numerical simulation, only the aft section (approximately 38% chord) of the model airfoil and the near wake are included in the computational domain, and the inlet Reynolds numbers based on the local momentum thickness and boundary-layer edge velocity are 2760 on the lower side and 3380 on the upper side. These values, obtained from an auxiliary RANS calculation, are used to emulate the experimental conditions at the LES inflow station, although some questions remain concerning their fidelity (Wang and Moin, 2000).

SIMULATION METHOD

The same energy-conserving finite difference scheme with dynamic subgrid-scale (SGS) stress model used for the wall-resolved LES (Wang and Moin, 2000) is employed. The computational domain is also identical to that of the full LES. It is of size $16.5h$, $41h$, and $0.5h$, where h denotes the airfoil thickness in the streamwise (x_1), wall-normal (x_2 or y), and spanwise (x_3) directions, respectively. The grid is coarsened to $768 \times 64 \times 24$, which is 1/6 of the original number of points. The first off-wall velocity nodes (on staggered mesh) are located at the lower edge of the logarithmic layer ($x_2^+ \approx 60$ for u_2 and $x_2^+ \approx 30$ for u_1 and u_3) near the computational inlet. The new grid is chosen to resolve the desired flow scales in the outer layer and is thus not strongly dependent on the Reynolds number. The total reduction in CPU time, due to both the smaller number of grid points and larger time steps, is over 90% compared to the full LES.

Since the simulation does not resolve the viscous sublayer, approximate wall boundary conditions are needed. They are imposed in terms of wall shear stress components τ_{wi} ($i = 1, 3$) determined from wall models of the form (Balaras et al., 1996; Cabot and Moin, 2000)

$$\frac{\partial}{\partial x_2}(\nu + \nu_t)\frac{\partial u_i}{\partial x_2} = F_i \qquad i = 1, 3 \qquad (1)$$

where

$$F_i = \frac{1}{\rho}\frac{\partial p}{\partial x_i} + \frac{\partial u_i}{\partial t} + \frac{\partial}{\partial x_j}u_i u_j \qquad (2)$$

The eddy viscosity ν_t is obtained from a RANS type mixing-length eddy viscosity model with near-wall damping (Cabot and Moin, 2000):

$$\frac{\nu_t}{\nu} = \kappa y_w^+ \left(1 - e^{-y_w^+/A}\right)^2 \qquad (3)$$

where $y_w^+ = y_w u_\tau / \nu$ is the distance to the wall in wall units (based on the local instantaneous friction velocity u_τ), κ is the model coefficient, and $A = 19$. The pressure in (2) is assumed x_2-independent, equal to the value from the outer-flow LES solution. Eqs. (1) and (2) are required to satisfy no-slip conditions on the wall and match the outer layer solutions at the first off-wall LES velocity nodes: $u_i = u_{\delta i}$ at $x_2 = \delta$.

Two simpler variants of the above wall model, with $F_i = 0$ and $F_i = \frac{1}{\rho}\frac{\partial p}{\partial x_i}$, are called equilibrium stress balance models (without and with pressure gradient). They are particularly easy to implement since (1) can be integrated to give a closed-form expression for τ_{wi} (Wang, 1999). If $F_i = 0$, the model implies the logarithmic law of the wall for the instantaneous velocities for $\delta^+ \gg 1$, and linear velocity distributions for $\delta^+ \ll 1$.

In the general case, however, the boundary layer equations (1)–(3) have to be solved numerically to obtain u_1 and u_3, and hence τ_{w1} and τ_{w3}. They are integrated in time along with the outer flow LES equations, using the same numerical scheme (fractional step in combination with the Crank-Nicolson method for the diffusion term and third order Runge-Kutta scheme for convective terms). The wall-normal velocity component u_2 is determined from the divergence-free constraint. Note that no pressure Poisson equation is required since pressure is assumed constant in the wall-normal direction. The grid for wall layer computation coincides with the LES grid in the wall-parallel directions. In the direction normal to the wall, 32 points are distributed uniformly between the airfoil surface and the

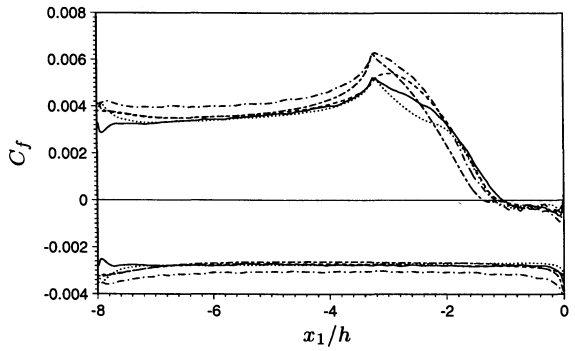

Figure 2: Distribution of the mean skin friction coefficient computed using LES with wall models given by (1). ---- $F_i = 0$; — - — $F_i = \frac{1}{\rho}\frac{\partial p}{\partial x_i}$; —·— $F_i = \frac{1}{\rho}\frac{\partial p}{\partial x_i} + \frac{\partial u_i}{\partial t} + \frac{\partial}{\partial x_j}u_i u_j$ and $\kappa = 0.4$; ——— $F_i = \frac{1}{\rho}\frac{\partial p}{\partial x_i} + \frac{\partial u_i}{\partial t} + \frac{\partial}{\partial x_j}u_i u_j$ and dynamic κ; ····· full LES (no wall model).

first off-wall velocity nodes for LES, with resolution of $\Delta x_2^+ \approx 1$ near the inlet. The computational cost for solving the boundary layer equations is insignificant compared with that for the outer layer LES because (1) there is no need to solve the x_2-momentum equation and the pressure Poisson equation, and (2), more importantly, the equations are solved in locally orthogonal coordinates instead of the general curvilinear coordinates used for the LES.

RESULTS AND DISCUSSION

Stress balance model

A good indicator of wall model performance is the prediction of the mean skin friction coefficient, which is shown in Fig. 2. The simple stress balance models, with $F_i = 0$ and $F_i = \frac{1}{\rho}\frac{\partial p}{\partial x_i}$ (dashed and chain-dashed lines respectively) and $\kappa = 0.4$ (the von Kármán constant), predict well the skin friction coefficient C_f on the lower surface (lower curves) and the flat section of the upper surface (upper curves). As the upper boundary-layer flow enters the region of strong favorable pressure gradient, the model with pressure gradient predicts better the qualitative behavior of C_f, including the peak location and the discontinuous slope at the peak, which corresponds to the intersection of the flat surface with the curved one (hence a discontinuity in surface curvature). Significant deviation between both model predictions and the full LES solution (dotted line) occurs downstream of the C_f peak, where the flow undergoes a favorable-to-adverse pressure gradient transition, suggesting that terms not included in the model, such as the convective terms, are important. It is worth noting that the separated region with negative C_f is predicted reasonably well by both stress balance models, because the near-wall layer is much thicker and hence resolved despite the coarse LES grid.

TBL equation model: the effect of model coefficient

The skin friction coefficient computed using the full TBL equations (1)–(3) and the standard von Kármán constant $\kappa = 0.4$ is plotted in Fig. 2 as the chain-dotted lines. It shows better qualitative trend than the stress balance model predictions. However, the magnitude is overpredicted in most regions, particularly on the flat surface, by up to 20%. This overprediction can be best explained as follows: If the streamwise component of (1) and (2) is integrated from the wall to $y = \delta$ and then time-averaged, one obtains

$$\begin{aligned}\overline{\tau}_{w1} &= \mu\frac{\partial U_1}{\partial x_2}\Big|_{x_2=0} \\ &= \frac{\rho}{\int_0^\delta \frac{dy}{\nu+\nu_t}}\left\{U_{\delta_1} - \frac{1}{\rho}\frac{\partial P}{\partial x_1}\int_0^\delta \frac{y dy}{\nu+\nu_t}\right. \\ &\quad \left. - \int_0^\delta \frac{1}{\nu+\nu_t}\int_0^y \frac{\partial}{\partial x_j}\overline{u_1 u_j}dy'dy\right\} \qquad (4)\end{aligned}$$

Note that to facilitate the analysis, ν_t has been treated as constant in the time-averaging as a first approximation. The first term in the curly brackets represents the wall shear stress from an equilibrium stress balance model without pressure gradient. The second term accounts for the mean pressure gradient effect, which contributes positively (negatively) to the wall shear stress under favorable (adverse) pressure gradient. The contribution from the nonlinear convective terms, represented by the last term in the brackets, can be easily shown to be positive in the case of a flat plate boundary layer. Hence, the inclusion of the nonlinear terms in the wall model equation increases the wall stress, causing the overprediction shown in Fig. 2 if contributions from other terms in (4) are not altered. To offset this increase, the only option is to reduce the turbulent eddy viscosity ν_t and hence the multiplication factor before the curly brackets in (4).

The physical explanation for requiring lower ν_t, as pointed out by Cabot and Moin (2000), is the fact that the Reynolds stress carried by the nonlinear terms in the boundary layer equations is significant. Hence, instead of modeling the total stress as in typical RANS calculations, the eddy-viscosity model is expected to account for only the unresolved part of the

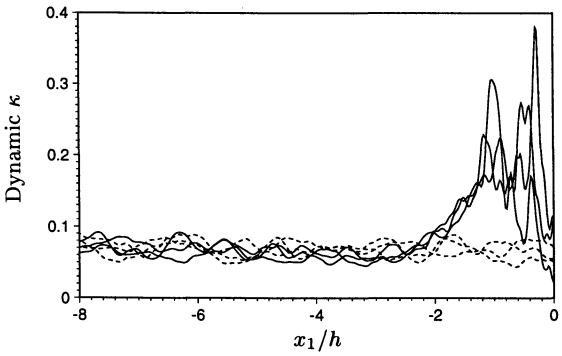

Figure 3: Dynamic κ for the mixing-length eddy viscosity model at three time instants. ——— upper side; ---- lower side.

Reynolds stress. Cabot and Moin (2000) suggested to compute the model coefficient dynamically by matching the stresses between the inner layer (wall model) and outer layer (LES) solutions. In the present calculation, the resolved portions of the nonlinear stresses from the inner and outer layer calculations are the same. To match the unresolved portions of the stresses approximately, we equate the mixing-length eddy viscosity to the SGS eddy viscosity at the matching points, $\langle \nu_t \rangle = \langle \nu_{sgs} \rangle$, from which the model coefficient κ is extracted using (3). The averaging denoted by the angular brackets is performed in the spanwise direction as well as over the previous 150 time steps to obtain reasonably smooth data. One difficulty with this method is that ν_{sgs} is poorly behaved at the first off-wall velocity nodes because the velocities at the wall are not well defined (we used slip velocities extrapolated from the interior nodes to compute the strain rate tensor and ν_{sgs}). As a practical matter, the matching points are moved to the second layer of velocity nodes from the wall instead.

The dynamically computed κ at three time instants is exemplified in Fig. 3, where the solid lines represent those on the upper side and dashed lines on the lower side. They are found to be only a small fraction of the standard value of 0.4. This figure indicates that on average, on the flat surfaces, only less than 20% of the Reynolds stress is modeled by the mixing-length eddy viscosity. The rest is directly accounted for by the the nonlinear terms in the wall layer equations. By using the reduced, variable model coefficient κ, the computed skin friction coefficient is much improved, as demonstrated by the solid line in Fig. 2. This dynamic modeling approach gives the best overall agreement with the results of the resolved LES compared with other wall models tested. This is true not only for the skin friction but also for other statistical quantities as well. Henceforth, only the solutions based on TBL equations with dynamic model coefficient will be presented.

Comparisons with full LES solutions

A comparison of the mean velocity predictions using LES with wall modeling and those from the full LES (Wang and Moin, 2000) is shown in Fig. 4. The velocity magnitude, defined as $U = (U_1^2 + U_2^2)^{1/2}$ and normalized by its value U_e at the boundary-layer edge, is plotted as a function of the vertical distance to the upper surface, at (from left to right) $x_1/h = -3.125, -2.125, -1.625, -1.125, -0.625$, and 0 (trailing-edge). With the exception of the trailing-edge point, these locations correspond to the measurement stations in Blake's (1975) experiment. The profiles obtained with wall modeling (solid lines) agree extremely well with the full LES profiles (dashed lines) at all stations, including those in the separated region which starts at $x_1/h = -1.125$. The agreement between both computational solutions and the experimental data is also reasonable, and the potential reasons for the observed discrepancies are discussed in Wang and Moin (2000).

Fig. 5 depicts the profiles of the rms streamwise velocity fluctuations at (from left to right) $x_1/h = -4.625, -2.125, -1.625, -1.125, -0.625$, and 0. Again, very good agreement between the present solutions and those of the full LES is observed, with the notable exception at $x_1/h = -1.125$, where the wall model solution agrees (perhaps fortuitously) better with the experiment.

In Fig. 6 the mean streamwise velocity profiles (normalized by free-stream velocity U_∞) are compared at select near-wake stations $x_1/h = 0$, 0.5, 1.0, 2.0, and 4.0. The solid lines are obtained from the present simulation, and the dashed lines are from the full LES. The corresponding rms streamwise velocity fluctuations are depicted in Fig. 7. The agreements between the LES solutions with and without wall modeling are good near the trailing-edge and deteriorate gradually in the downstream direction. This is caused by the much reduced grid resolution in the case of LES with wall modeling. The grid has been coarsened by the same factor in the wake as in the wall bounded region, even though the wall model does not play a role there. Apparently, this has caused insufficient grid resolution, particularly in the

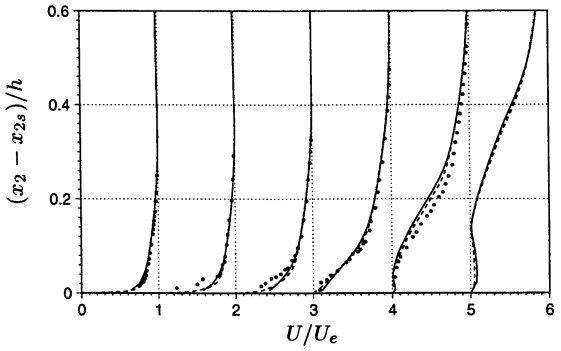

Figure 4: Profiles of the normalized mean velocity magnitude as a function of vertical distance to the upper surface, at (from left to right) $x_1/h = -3.125, -2.125, -1.625, -1.125, -0.625$, and 0 (trailing-edge). ——— LES with wall model; - - - - full LES; • Blake's experiment.

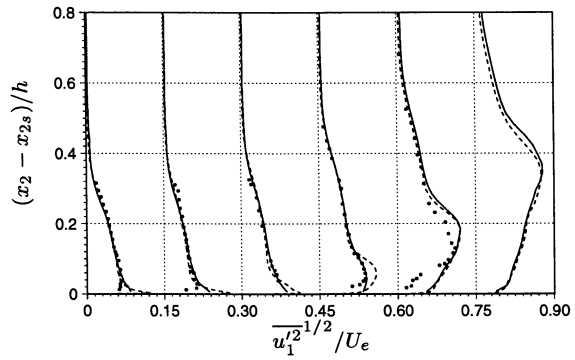

Figure 5: Profiles of the rms streamwise velocity fluctuations as a function of vertical distance to the upper surface, at (from left to right) $x_1/h = -4.625, -2.125, -1.625, -1.125, -0.625$, and 0 (trailing-edge). ——— LES with wall model; - - - - full LES; • Blake's experiment.

streamwise and spanwise directions.

Of particular interest in aeronautical and naval applications is the predictive capability of LES with wall modeling for surface pressure fluctuations. A preliminary assessment is given in Fig. 8, which depicts the frequency spectra of the unsteady surface pressure at select stations in the favorable (Fig. 8a) and adverse (Fig. 8b) pressure gradient regions, at the separation point (Fig. 8c), and inside the separated region (Fig. 8d). The variable q_∞ used in the normalization is the dynamic pressure, defined as $\rho U_\infty^2/2$. Relative to Blake's experimental data, the pressure spectra from the simulation employing the wall model are of comparable accuracy as those from the full LES, although the resolvable frequency ranges are narrower due to the coarser grid. However, relative to the full LES spectra, the spectral levels are somewhat overpredicted. This phenomenon has also been observed previously in channel flow LES with wall models. The discrepancies may be attributable to the approximation of

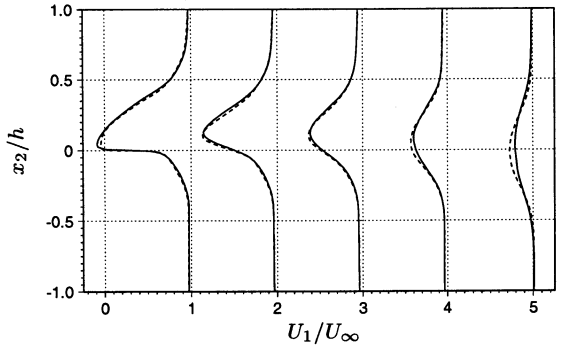

Figure 6: Profiles of the normalized mean streamwise velocity in the wake, at (from left to right) $x_1/h = 0, 0.5, 1.0, 2.0$, and 4.0. ——— LES with wall model; - - - - full LES.

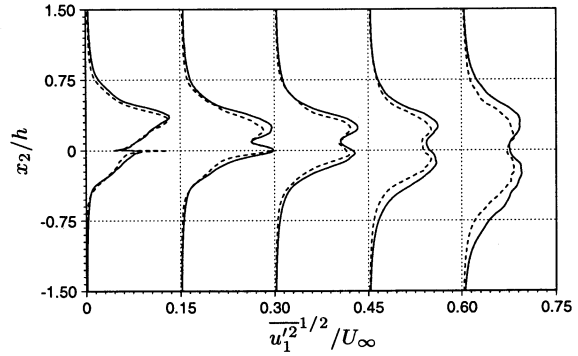

Figure 7: Profiles of the rms streamwise velocity fluctuations in the wake, at (from left to right) $x_1/h = 0, 0.5, 1.0, 2.0$, and 4.0. ——— LES with wall model; - - - - full LES.

wall pressure by the cell-centered values adjacent to the wall and the fact that in the present LES formulation the "pressure" actually contains the subgrid-scale kinetic energy. The latter is negligibly small at the first off-wall pressure node if the wall layer is resolved but may not be negligible in the present case because of the coarse mesh. This issue needs to be examined in future studies.

CONCLUSIONS

In summary, we have examined the efficacy of LES with wall modeling for complex wall-bounded flows by considering turbulent boundary layer flows past an asymmetric trailing-edge. It is demonstrated that when a RANS type eddy viscosity is used in wall-layer equations that contain nonlinear convective terms, its value must be reduced to account for only the unresolved part of the Reynolds stress. This is important for all flows, particularly attached flows. A dynamically adjusted wall-model eddy viscosity is employed in the TBL equation model, which is shown to be considerably more accurate than the simpler algebraic models based on the instantaneous log

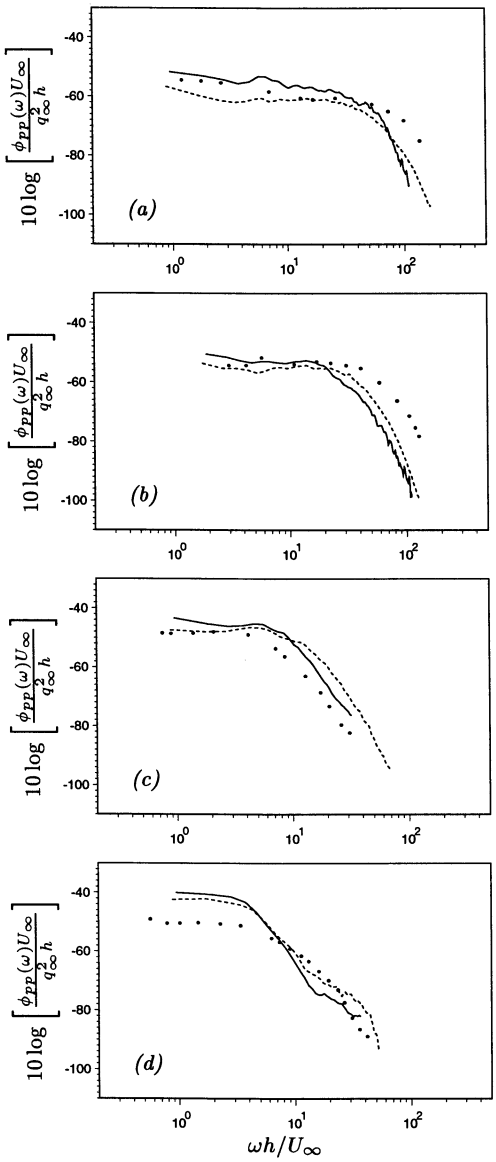

Figure 8: Frequency spectra of pressure fluctuations on the upper surface at x_1/h = (a) -3.125, (b) -1.625, (c) -1.125, and (d) -0.625. ——— LES with wall model; - - - - full LES; • Blake's experiment.

law. This modeling approach predicts low-order velocity statistics in very good agreement with those from the full LES, at a small fraction of the original computational cost. In particular, the unsteady separation near the trailing-edge is captured correctly, and the surface pressure spectra also appear promising. The effect of wall-modeling on the predictions of surface pressure fluctuations and acoustic radiation will be examined and quantified in future investigations.

ACKNOWLEDGMENTS

We would like to thank P. Bradshaw, W. Cabot, and J. Jiménez for valuable discussions during the course of this work. This research was supported by the U. S. Office of Naval Research under Grant N00014-95-1-0221. Computations were carried out on the NAS facilities at NASA Ames Research Center and on facilities at the DoD Major Shared Resource Center/Aeronautical Systems Center.

REFERENCES

Baggett, J. S., Jiménez, J., and Kravchenko, A. G., 1997, "Resolution Requirements in Large-Eddy Simulations of Shear Flows", *Annual Research Briefs*, Center for Turbulence Research, NASA Ames/Stanford Univ., pp. 51–66.

Balaras, E., Benocci, C., and Piomelli, U., 1996, "Two-Layer Approximate Boundary Conditions for Large-Eddy Simulation", *AIAA Journal*, Vol. 34, pp. 1111–1119.

Blake, W. K., 1975, "A Statistical Description of Pressure and Velocity Fields at the Trailing Edge of a Flat Strut", DTNSRDC Report 4241, David Taylor Naval Ship R & D Center, Bethesda, Maryland.

Cabot, W. and Moin, P., 2000, "Approximate Wall Boundary Conditions in the Large-Eddy Simulation of High Reynolds Number Flow", *Flow, Turbulence and Combustion*, Vol. 63, pp. 269–291.

Grötzbach, G., 1987, "Direct Numerical and Large Eddy Simulation of Turbulent Channel Flows", In *Encyclopedia of Fluid Mechanics*, N. P. Cheremisinoff ed., Gulf Pub. Co., Chap. 34, pp 1337–1391.

Piomelli, U., Ferziger, J., Moin, P., and Kim, J., 1989, "New Approximate Boundary Conditions for Large Eddy Simulations of Wall-Bounded Flows", *Physics of Fluids*, Vol. 1, pp. 1061–1068.

Schumann, U., 1975, "Subgrid Scale Model for Finite Difference Simulations of Turbulent Flows in Plane Channels and Annuli", *Journal of Computational Physics*, Vol. 18, pp. 376–404.

Wang, M., 1999, "LES with Wall Models for Trailing-Edge Aeroacoustics", *Annual Research Briefs*, Center for Turbulence Research, NASA Ames/Stanford Univ., pp. 355–364.

Wang, M. and Moin, P., 2000, "Computation of Trailing-Edge Flow and Noise Using Large-Eddy Simulation", *AIAA Journal*, Vol. 38, pp. 2201–2209.